

This relation is plotted in Fig. 2. It is noteworthy that with moderate mass flow ratios the total pressure of the outflowing secondary flow can be considerably higher than that of the inflowing primary. This points to the possibility of promising looped arrangements (turbocompressors, gas generators, turbojets) in which some or all of the extracted secondary flow is energized through heat addition to form the primary source.

These results are in general agreement with those obtained by a different procedure in Ref. 2, for fully looped systems, with consideration of compressibility effects.

### References

<sup>1</sup> Foa, J. V., "A note on a method of energy exchange," *ARS J.* **32**, 1396-1398 (1962).

<sup>2</sup> Foa, J. V., "A new method of energy exchange between flows and some of its applications," *Rensselaer Polytechnic Institute TR AE 5509* (December 1955).

## Preliminary Orbit Determination for a Moon Satellite from Range-Rate Data

Z. E. SCHWARZBEIN\* AND ROBERT H. GERSTEN†  
*Northrop Corporation, Hawthorne, Calif.*

### Derivation

SEVERAL of the manned lunar missions planned for this decade require the establishment of selenocentric orbits. The data for determining these orbits may originate from 1) earth-based observations, 2) a base on the moon, 3) another vehicle on a definitive selenocentric orbit, or 4) the orbiting vehicle itself. Because of the large separation distances involved, the first alternative is, at present, impractical. Likewise, since neither a moon base nor a selenocentric satellite on a definitive orbit from which observations can be made will be established for the early missions, alternatives 2 and 3 are not considered. For these reasons, a method based upon the fourth alternative is presented here.

Preliminary determination of the position and velocity of a selenocentric orbiting vehicle is obtained from two measurements of range-rate (vertical to the lunar surface), vehicular sublatitude, sublongitude, and the time separation between these measurements. The determination of sublatitude and sublongitude points can be accomplished by recognizing lunar landmarks and associating them with their proper selenocentric coordinates and/or by use of stellar observations. The former method is, of course, greatly dependent upon progress in knowledge of the lunar cartography. The computations can be performed by either an on-board or earth-based computer. A mathematical model using two-body analysis throughout is described in this paper. Like the modified Gaussian procedure of orbit determination from two positions and time of flight developed by Herrick and Liu,<sup>1-3</sup> this method requires iteration upon assumed values of the parameter  $p$  (semilatus rectum). However, although in the former method a unique true anomaly is obtained for each assumed  $p$ , in this method the value of the true anomaly is independent of the parameter, a fact that results in a less complex iteration procedure.

Received by ARS August 29, 1962; revision received November 19, 1962.

\* Member of the Technical Staff, Astrodynamics Branch, Analytical Group, Northrop Space Laboratories.

† Member of the Technical Staff, Astrodynamics Branch, Analytical Group, Northrop Space Laboratories. Member AIAA.

The following inertial coordinate system is adopted. The origin of coordinates is taken as the geometric center of the moon with the  $x$  and  $y$  axes lying in the lunar equator plane and the  $z$  axis directed toward the lunar north pole. The  $x$  axis is coincident with the intersection of the lunar prime meridian with the lunar equator at the time of the first observation, taken as positive toward the earth. The sense of the  $y$  axis is such that  $x, y, z$  forms a right-handed set (see Fig. 1).

The unit vectors  $\mathbf{U}_1$  and  $\mathbf{U}_2$  directed from the origin to the satellite at the observation times are given by

$$\mathbf{U}_1 = \cos\phi_1 \cos\lambda_1 \mathbf{i} + \cos\phi_1 \sin\lambda_1 \mathbf{j} + \sin\phi_1 \mathbf{k} \quad (1)$$

$$\mathbf{U}_2 = \cos\phi_2 \cos[\lambda_2 + \dot{\theta}_c (t_2 - t_1)] \mathbf{i} + \cos\phi_2 \sin[\lambda_2 + \dot{\theta}_c (t_2 - t_1)] \mathbf{j} + \sin\phi_2 \mathbf{k} \quad (2)$$

where  $\mathbf{i}, \mathbf{j}, \mathbf{k}$  are unit vectors in the  $x, y, z$  directions, respectively,  $\dot{\theta}_c$  is the rotation rate of the moon,  $\phi$  and  $\lambda$  represent the lunar sublatitude and sublongitude, respectively,  $t$  is the observation time, and the subscripts 1 and 2 correspond to the first and second observations. For this analysis the

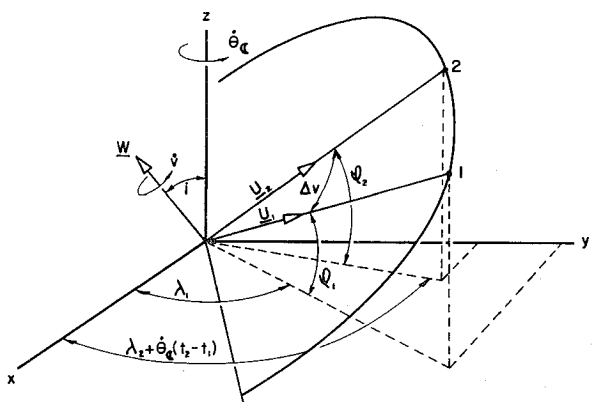


Fig. 1 Inertial coordinate system

longitude is measured as positive in the direction of the moon's rotation with  $0^\circ$  longitude located along the prime meridian.

The increment in true anomaly  $\Delta v$  between the forementioned vectors is given by the dot product

$$\begin{aligned} \mathbf{U}_1 \cdot \mathbf{U}_2 &= \cos(v_2 - v_1) = \cos\Delta v \\ &= \cos\phi_1 \cos\phi_2 \cos\lambda_1 \cos[\lambda_2 + \dot{\theta}_c (t_2 - t_1)] \\ &\quad + \cos\phi_1 \cos\phi_2 \sin\lambda_1 \sin[\lambda_2 + \dot{\theta}_c (t_2 - t_1)] \\ &\quad + \sin\phi_1 \sin\phi_2 \end{aligned} \quad (3)$$

For this analysis, the assumption is made that  $0 < \Delta v < \pi$ . In view of the present lack of knowledge of landmarks on the back side and limbs of the moon, this assumption is felt to be valid. Thus  $\Delta v$  may be assigned to the first or second quadrant and uniquely determined from Eq. (3).

The radial velocities  $\dot{r}$  at the observation times satisfy the following relations:

$$\dot{r}_1 = (\mu/p)^{1/2} e \sin v_1 \quad (4a)$$

$$\dot{r}_2 = (\mu/p)^{1/2} e \sin(v_1 + \Delta v) \quad (4b)$$

where  $e$  is the orbital eccentricity,  $p$  is the parameter (semilatus rectum), and  $\mu$  is the product of the universal gravitational constant and the mass of the moon or the product of the gravitational acceleration at the moon's surface and the square of the (assumed constant) lunar radius. Since the triaxiality of the moon and local anomalies are neglected in this analysis, the measured range-rate may be set equal to  $\dot{r}$ . From Eqs. (4a) and (4b) one can obtain, after some manip-

ulation, the value of the true anomaly at the first observation time:

$$\tan v_1 = \frac{\dot{r}_1}{(\dot{r}_2 - \dot{r}_1 \cos \Delta v) \csc \Delta v} \quad (5)$$

In assigning the proper quadrant to  $v_1$ , the signs of the numerator and denominator are equal, respectively, to the signs of  $\sin v_1$  and  $\cos v_1$ . The true anomaly associated with the second point is obtained directly from

$$v_2 = v_1 + \Delta v \quad (6)$$

At this point it is necessary to make initial estimates of the parameter  $p$ . For each of these estimates, the associated orbital eccentricity is computed from

$$e = \left\{ \frac{p}{\mu} \left[ \dot{r}_1^2 + \left( \frac{\dot{r}_2 - \dot{r}_1 \cos \Delta v}{\sin \Delta v} \right)^2 \right] \right\}^{1/2} \quad (7)$$

which is obtained from (4a) and (4b). The time equation is given by<sup>4</sup>

$$(t_2 - t_1)_c = \left( \frac{p^3}{\mu} \right)^{1/2} \frac{1}{1 - e^2} \left\{ \frac{-e \sin v}{1 + e \cos v} + \frac{2}{(1 - e^2)^{1/2}} \tan^{-1} \left[ \left( \frac{1 - e}{1 + e} \right)^{1/2} \tan \frac{v}{2} \right] \right\}_{v_1}^{v_2} \quad (8)$$

where the subscript  $c$  indicates a computed value. This equation is valid for circular and elliptical orbits. In general, the computed and measured flight times will not agree initially to the accuracy desired. In this case, it is necessary to iterate on Eq. (8) to obtain a new estimate for  $p$  and return to Eq. (7) to compute the associated orbital eccentricity. This procedure is repeated until the computed and measured flight times agree to the accuracy desired.

One now has sufficient information to determine the position and velocity at the first observation time in the inertial coordinate system selected. This can be accomplished in two steps. The first step involves determination of the triad of unit vectors  $\mathbf{U}_1, \mathbf{V}_1, \mathbf{W}$ , where  $\mathbf{U}_1$  is directed from the origin of coordinates to the vehicle at the first observation time,  $\mathbf{W}$  is normal to the orbit plane in the direction of the moment of momentum vector, and  $\mathbf{V}_1$  lies in the orbit plane such that  $\mathbf{U}_1, \mathbf{V}_1, \mathbf{W}$  form a right-handed set. The unit vector orthogonal to the orbital plane  $\mathbf{W}$  is given by

$$\mathbf{W} = (\mathbf{U}_1 \times \mathbf{U}_2) / |\mathbf{U}_1 \times \mathbf{U}_2| \quad (9)$$

From  $\mathbf{W}$  and  $\mathbf{U}_1$ , the unit vector  $\mathbf{V}_1$  is obtained by

$$\mathbf{V}_1 = \mathbf{W} \times \mathbf{U}_1 \quad (10)$$

The second step consists of calculating the separation of the vehicle from the dynamical center  $r_1$  and the transverse component of velocity  $(rv)_1$  at the time of the first observation from

$$r_1 = p / (1 + e \cos v_1) \quad (11)$$

and

$$(rv)_1 = (\mu p)^{1/2} / r_1 \quad (12)$$

Using the foregoing values, the position vector  $\mathbf{r}_1$  and velocity vector  $\dot{\mathbf{r}}_1$  at the time of the first observation are given by

$$\mathbf{r}_1 = r_1 \mathbf{U}_1 \quad (13)$$

and

$$\dot{\mathbf{r}}_1 = \dot{r}_1 \mathbf{U}_1 + (rv)_1 \mathbf{V}_1 \quad (14)$$

The last two equations uniquely define the two-body orbit in inertial space.

### The circular orbital case

Since it is assumed that  $0 < \Delta v < 180^\circ$ , if the measured value of  $\dot{r}_1$  and  $\dot{r}_2$  are both equal to zero, the orbit may be assumed to be circular. In this case Eqs. (5) and (6) are replaced by  $v_1 = 0$  and  $v_2 = \Delta v$ . (This assumption is valid since the true anomaly is not defined for circular orbits.) In addition, the iteration procedure becomes unnecessary, and  $p$  is obtained directly by replacing Eq. (8) with

$$p = \{ [(t_2 - t_1) / \Delta v]^2 \mu \}^{1/3}$$

Also, Eqs. (11) and (12) are replaced with  $r_1 = p$  and  $(rv)_1 = (\mu / r)^{1/2}$ .

### Numerical example

In order to test the method presented in the foregoing, an orbit having the following characteristics is considered:  $a = 6,842,700$  ft;  $e = 0.1$ ;  $\omega = 30^\circ$ ;  $\Omega = 45^\circ$ , where  $a$ ,  $\omega$ , and  $\Omega$  are the semimajor axis, argument of periselene, and argument of the ascending node, respectively. It is further assumed that the sublatitude and sublongitude of the first observation are  $\phi_1 = 30^\circ$  and  $\lambda_1 = 90^\circ$  and that the separation in true anomaly between the two observations is  $\Delta v = 90^\circ$ . The foregoing quantities uniquely determine the second set of sublatitude and sublongitude points and the time increment between observation as  $\phi_2 = 22.0^\circ 787$ ;  $\lambda_2 = 193.0^\circ 734$ ;  $t_2 - t_1 = 32.918$  min and the orbital inclination  $i$  as  $i = 39.0^\circ 232$ .

The simulated "measurements" of range-rate associated with these "observations" are  $\dot{r}_1 = 191.25$  fps and  $\dot{r}_2 = 467.73$  fps. This orbit exhibits the following inertial components of position and velocity at the first observation time:

$$\begin{cases} x_1 = 0 \\ y_1 = 5,369,700 \text{ ft} \\ z_1 = 3,100,200 \text{ ft} \end{cases} \quad \begin{cases} \dot{x}_1 = -4938.1 \text{ fps} \\ \dot{y}_1 = -1068.9 \text{ fps} \\ \dot{z}_1 = 2233.9 \text{ fps} \end{cases}$$

The simulated values of  $\dot{r}_1, \dot{r}_2, \phi_1, \lambda_1, \phi_2, \lambda_2$ , and  $(t_2 - t_1)$  given are substituted in the derived equations. In order to initiate the iteration procedure, the values  $p = 8,370,400$  ft and  $6,377,800$  ft were selected. Two successive applications of Newton's iteration procedure yielded the following initial conditions

$$\begin{cases} x_1 = 0 \\ y_1 = 5,372,300 \text{ ft} \\ z_1 = 3,101,700 \text{ ft} \end{cases} \quad \begin{cases} \dot{x}_1 = -4937.0 \text{ fps} \\ \dot{y}_1 = -1068.6 \text{ fps} \\ \dot{z}_1 = 2233.4 \text{ fps} \end{cases}$$

### Method for obtaining the second initial estimate of $p$ and proof of the uniqueness of the solution

Since the first value of the parameter  $p$  is completely random, it is desirable to obtain an "educated" second estimate of  $p$ . In order to accomplish this, the variation of transfer time with  $p$  for this family of orbits (ellipses having fixed values of true anomaly and radial velocity at the observation points) is investigated. The radial velocities at the observation points are given by Eqs. (4a) and (4b). Assume a reference orbit having the same values of true anomaly and radial velocity at the observation points. For this latter orbit, one can write

$$\dot{r}_1 = (\mu / p_0)^{1/2} e_0 \sin v_1 \quad (15a)$$

$$\dot{r}_2 = (\mu / p_0)^{1/2} e_0 \sin(v_1 + \Delta v) \quad (15b)$$

where the subscript 0 indicates elements of the reference orbit. Combining Eqs. (4a) and (15a) or (4b) and (15b) yields

$$e = K_1 p^{1/2} \quad (16)$$

where  $K_1 = e_0 / p_0^{1/2}$  is a positive constant. Combining Eqs. (11) and (12) for a generalized point and integrating between fixed values of true anomaly, one obtains

$$t_2 - t_1 = \int_{v_1}^{v_2} \left( \frac{p^3}{\mu} \right)^{1/2} \frac{dv}{(1 + e \cos v)^2} \quad (17)$$

Substituting (16) into (17) gives

$$t_2 - t_1 = \int_{v_1}^{v_2} F(p, v) dv \quad (18)$$

where

$$F(p, v) = \left( \frac{p^3}{\mu} \right)^{1/2} \frac{1}{(1 + K_1 p^{1/2} \cos v)^2} \quad (19)$$

In order that the transfer time given by Eq. (18) increase (or decrease) with  $p$ , it is sufficient that  $F(p, v)$  increase (or decrease) monotonically with  $p$  for all values of  $v$  in the interval considered. Differentiating (19) with respect to  $p$  and remembering Eq. (16) yields

$$\frac{\partial F(p, v)}{\partial p} = \frac{1}{2} \left( \frac{p}{\mu} \right)^{1/2} \frac{3 + e \cos v}{(1 + e \cos v)^3} \quad (20)$$

which is always positive for elliptical orbits.

Hence, it is shown that the time interval increases monotonically with  $p$ . Thus, if the initial estimate for  $p$  yields a time of flight greater (less) than the observed time increment, the second estimate is lowered (raised) relative to the first. The foregoing procedure may be used to obtain values of  $p$  yielding times of flight bounding the observed increment. These values then may be used as initial estimates for the iteration procedure. The foregoing constitutes a proof of the uniqueness of the solution, i.e., each  $p$  is associated with one and only one time of flight.

#### References

- 1 Herrick, S., *Astrodynamics* (D. Van Nostrand Co. Inc., Princeton, N. J., to be published).
- 2 Liu, A., "Two-body orbit determination from two positions and time of flight," Aeroneutronic Interim TN 4 (January 2, 1959).
- 3 Baker, R. M. L., Jr. and Makemson, M. W., *An Introduction to Astrodynamics* (Academic Press, Inc., New York, 1960), pp. 137-139.
- 4 Plummer, H. C., *An Introductory Treatise on Dynamical Astronomy* (Dover Publications Inc., New York, 1960), p. 24.

## Resonance Scattering Photography of Free Molecular Flow

WALTER VALI\* AND GEORGE M. THOMAS†

Lockheed Missiles and Space Company, Palo Alto, Calif.

An experiment is described in which the free molecular flow of sodium vapor from an orifice was photographed, using the resonance scattering technique. The Knudsen number in the upstream chamber based on the orifice diameter was about 40. Photographs are presented of the flow over a cylinder and a plate.

#### Introduction

THE resonance scattering technique for visualizing flow makes it possible to obtain photographs at density levels several orders of magnitude lower than with previous techniques.<sup>1</sup> Application of this technique to a simple free

Received by ARS September 10, 1962.

\* Consultant; permanent address, Stanford University, Stanford, Calif.

† Member, Mechanical and Mathematical Sciences Laboratory.

molecular flow in which the properties of the flow field are known is desirable. The effusion of gas from a container into vacuum through an orifice is such a flow. The properties of free jet issuing from the orifice may be calculated quite accurately from simple kinetic theory considerations.<sup>2</sup> Another advantage of this flow is that, simply by changing the upstream density, the jet flow may be varied from continuum to free molecule. This note describes an experiment that was devised to illustrate the use of resonance scattering for visualizing free molecular orifice flow.

#### Theory of Resonance Scattering

The present method for observing low density gas flow (number of atoms per cubic centimeter between  $10^7$  and  $10^{12}$ ) is based on the knowledge that the scattering cross section of photons close to resonance becomes very large. The intensity of scattered radiation compared to the incident intensity is<sup>3</sup>

$$I/I_0 = \phi(\theta)/R^2 \quad (1)$$

where  $I$  and  $I_0$  are the scattered and incident intensities,  $R$  is the distance to the scattering center, and  $\phi$ , for classical elastically bound electrons, is

$$\phi(\theta) = \frac{e^2}{mc^2} \frac{\nu^4 \sin^2(\theta)}{(\nu_0^2 - \nu^2)^2 + \nu^2 \gamma^2} \quad (2)$$

Here  $e$  is electronic charge,  $m$  electron mass,  $c$  velocity of light,  $\nu$  frequency of incident light,  $\nu_0$  frequency of resonance light, and

$$\gamma = 2e^2 \nu_0^2 / 3mc^3 \quad (3)$$

Thus the total classical scattering cross section can be obtained by integrating Eq. (2) over a sphere:

$$\phi_{\text{total}} = \frac{8\pi}{3} \frac{e^4}{m^2 c^4} \frac{\nu^4}{(\nu_0^2 - \nu^2)^2 + \nu^2 \gamma^2} \quad (4)$$

This can be approximated for the immediate neighborhood of resonance as

$$\phi_{\text{total}} = \frac{2\pi e^4}{3m^2 c^4} \frac{\nu^2}{(\nu_0 - \nu)^2 + (\gamma^2/4)} \quad (5)$$

Quantum mechanical treatment of the scattering process introduces only a moderate correction. Thus, it is found that the total cross section of light exactly at resonance is

$$\phi_{\text{total}} = \lambda^2 / 2\pi \quad (6)$$

where  $\lambda$  is the wavelength of the resonance light. For the present application of sodium *D* lines to low density and low temperature sodium vapor, the scattering cross section is

$$\phi_{\text{total}} \approx (6 \times 10^{-5})^2 / 6 = 6 \times 10^{-10} \text{ cm}^2$$

Therefore a density of sodium atoms of  $10^9 \text{ cm}^{-3}$  will scatter a large fraction of the incident light. Densities of the order of  $10^7$  particles/cm<sup>3</sup> should be observable by the resonance scattering method.

#### Free Molecular Effusion

Consider the free molecular effusion of sodium atoms through a small orifice of diameter  $d$  and negligible lip thickness. The flow may be considered free molecular if the mean free path  $\Lambda$  in the container is large compared to  $d$ . The number of atoms per unit time escaping the orifice is therefore

$$N_i = \frac{1}{4} \bar{C} N_0 A \quad (7)$$

where

$$\bar{C} = (3KT_0/m)^{1/2} = \text{mean molecular velocity upstream of the orifice}$$

$$N_0 = \text{number of atoms per unit volume in the source}$$

$$T_0 = \text{temperature of the source}$$